

## MORPHOTECTONIC ANALYSIS OF HERAKLION BASIN (CRETE, GREECE)

Kokinou E.<sup>1</sup>, Skilodimou H. D.<sup>2</sup> and Bathrellos G.D.<sup>2</sup>

<sup>1</sup> *Technological Educational Institute Crete, Department of Natural Resources & Environment,  
Chania, Crete, Greece, ekokinou@chania.teicrete.gr*

<sup>2</sup> *National & Kapodistrian University of Athens, Faculty of Geology & Geoenvironment, Depart-  
ment of Geography & Climatology, University Campus, Zografou, ZC 15784, Athens, Greece,  
hskilodimou@geol.uoa.gr, gbathrellos@geol.uoa.gr*

### Abstract

*In the present study, geomorphological, geological data and morphotectonic analysis were combined in order to investigate the relation between the tectonic activity and the geomorphology in the Heraklion basin (Crete). GIS techniques were used for mapping the various topographic, geological and tectonic features of the study area. The digital elevation model (DEM) of the study area was created. The slope angle and aspect maps were derived from DEM and combined with fault system orientation. The influence of tectonism on the development of drainage system was examined by the comparison of fault and stream directions. Moreover, geomorphic indices are useful tools in evaluating tectonic activity, relating the sensitivity to rock resistance, climatic change and tectonic processes with the production of a certain landscape. The applied geomorphic indices, in the present study, are the mountain front sinuosity index ( $S_{mf}$ ) and the valley floor width to valley height ratio ( $V_f$ ). The fault zones of the study area are generally oriented N-S, NE-SW, NW-SE and E-W. According to the morphological analysis, steep slopes and sudden changes corresponding to the azimuth of the slope direction, are mainly related to N-S, NNE-SSW and NNW-SSE oriented faulting. The main channel directions of the drainage system are mainly controlled by faults striking N-S. The E-W, NE-SW and NW-SE general trending fault systems affect the low order streams. The  $S_{mf}$  and  $V_f$  values are low, implying that the tectonic activity influences the morphology of the study area. The above methodology was proved successful to examine the impact of the tectonic activity in the study area.*

**Key words:** *Geomorphic indices, GIS, fault.*

### Περίληψη

*Στόχος της παρούσας εργασίας είναι να συνδυάσει τα γεωλογικά δεδομένα με την μορφολογική και μορφοτεκτονική ανάλυση με στόχο να καθοριστεί η επίδραση της τεκτονικής στην διαμόρφωση του επιφανειακού αναγλύφου για τμήμα της λεκάνης του Ηρακλείου στην Κρήτη. Τα Γεωγραφικά Συστήματα Πληροφοριών χρησιμοποιήθηκαν για να απεικονιστούν τα τοπογραφικά, γεωλογικά και τεκτονικά δεδομένα της περιοχής. Αρχικά δημιουργήθηκε το ψηφιακό μοντέλο υψομέτρων και στην συνέχεια προέκυψαν από αυτό ο χάρτης κλίσεων και ο χάρτης προσανατολισμού και συνδυάστηκαν με το τεκτονικό σύστημα της περιοχής. Η επίδραση του τεκτονισμού στην ανάπτυξη*

του υδρογραφικού δικτύου εκτιμήθηκε, λαμβάνοντας υπόψιν τον προσανατολισμό των ρηγματίων και των ρεμάτων. Επιπρόσθετα στα πλαίσια της παρούσας εργασίας προσδιορίστηκαν δύο μορφοτεκτονικοί δείκτες με στόχο να αξιολογηθεί η τεκτονική δραστηριότητα της περιοχής. Αυτοί αντιστοιχούν στον δείκτη ευθυγράμμισης του ορεογραφικού μετώπου ( $S_{mf}$ ) και στον δείκτη λόγου πλάτους κοιλάδας προς ύψος κοιλάδας ( $V_f$ ). Τα ρήγματα της περιοχής παρουσιάζουν γενικά προσανατολισμό B-N, BA-ND, BA-NA και A-Δ. Από την μορφολογική ανάλυση προκύπτει ότι οι απότομες κλίσεις καθώς και οι απότομες μεταβολές προσανατολισμού σχετίζονται με τα ρήγματα διεύθυνσης B-N, BBA-NNA και BBA-NNA. Οι κύριοι κλάδοι του υδρογραφικού δικτύου πιθανόν ελέγχονται από τα ρήγματα γενικής διεύθυνσης B-N. Οι δείκτες  $S_{mf}$  και  $V_f$  παρουσιάζουν χαμηλές τιμές, γεγονός που δείχνει ότι η μορφολογία της περιοχής έχει επηρεαστεί σε μεγάλο βαθμό από την τεκτονική δραστηριότητα. Η παραπάνω μεθοδολογία ανάλυσης αποδείχθηκε επιτυχής στους στόχους που έθεσε η παρούσα εργασία.

**Λέξεις κλειδιά:** Μορφοτεκτονικοί δείκτες, Γ.Σ.Π., ρήγμα.

## 1. Introduction

The wide area of Heraklion city is located in the Heraklion basin (Figure 1A), comprising a large Neogene basin (900 km<sup>2</sup>) in central Crete. The Neogene deposits of Heraklion basin overlie basement rocks of the Upper Nappes (Gavrovo-Tripolis, Pindos and the heterogeneous Uppermost Unit). The Upper Nappes are separated from the HP-LT metamorphic rocks of the Lower Nappes (parautochthone Plattenkalk and Phyllite-Quartzite units) by the Cretan detachment (Zachariasse et al., 2011; Kokinou et al., 2012). This fault (or faults) is in many places exposed with a sense of shear either to both S and N (Kilias et al., 1994; Fassoulas, 1999), or dominantly top-to the north (Jolivet et al., 1996).

The evolution of a complex landscape is the result of the interactions involving climate, tectonic and surface progress. Therefore the study of the geomorphological features such as the drainage may assist in understanding the landscape evolution and recognize active tectonic movements (Riquelmea et al., 2003; Malik and Mohanty, 2007; Bathrellos et. al., 2009, Kamberis et al., 2012).

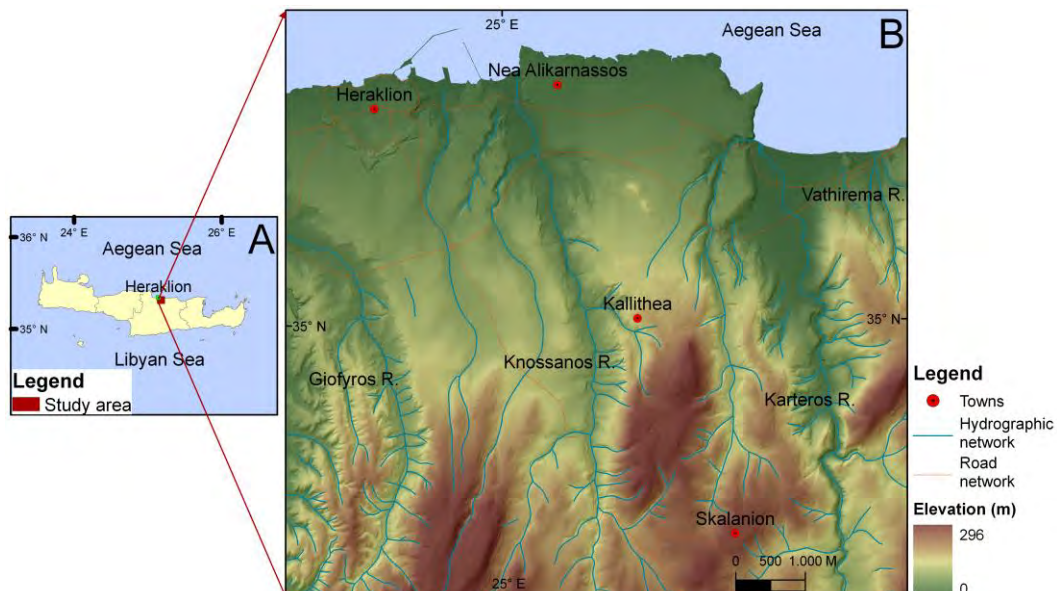


Figure 1 - A: Map of Crete showing the study area, B: Elevation map of the study area.

Several studies have proposed that the investigation of geomorphological features and geomorphic indices such as the mountain front sinuosity ( $S_{mf}$  index) and the valley floor width to valley height ratio ( $V_f$  index) provide useful information regarding the influence of tectonics on landscape evolution (e.g. Bull and McFadden, 1977; Rockwell et al., 1984; Keller, 1986; Burbank and Anderson, 2001; Theocharis and Fountoulis, 2002; Silva et al., 2003; Tsodoulos et al., 2008).

The main scope of the present study is to combine geomorphological, geological data and morphotectonic analysis in order to investigate the relation between the tectonic activity and the geomorphology in the Heraklion basin (Crete).

## **2. Geology of the Study Area**

The Heraklion's basin comprises an almost flat area (maximum elevation at 296m) with the exception of some hilly areas, showing an extended development of the drainage. The rivers of the basin flow from South to North into Aegean Sea (Figure 1B).

The geological map (Figure 2) of the study area was created, based on the existing geological map (IGME, 1:50,000) and field observations.

The Heraklion's basin is mainly filled by fluvial and marine sediments of Holocene, Pleistocene, Lower-Middle Pliocene, Upper Miocene, Cretaceous – Middle Eocene and Upper Triassic-Upper Jurassic (Figure 2). The Holocene sediments (al) mainly comprise fluvial and closed basin deposits, situated in the western part of the city, on either side of the drainage network. Pleistocene–Holocene sediments (Qs) are generally located across the coastline, comprising of undivided marine terraces and coastal sands. The Pleistocene Heraklion formation (Pt) consists of marine bioclastic limestones, sandstones with cross-bedded conglomerates and marls. The majority of the basin's interior consists of Lower-Middle Pliocene sediments (Pl.m), comprising of white marls or marly limestones, grayish clays with brown, often thin bedded intercalations, white beige fossiliferous marls, laminated marls or diatomites and bioclastic limestones. The base of this formation consists in general of an unsorted "marly breccia". It overlies unconformably the Upper Miocene formation (M.k), consisting of bioclastic, reef limestones, marls or marly limestones (M.m) and gypsum (g). In the eastern part of Heraklion are situated Cretaceous–Middle Eocene (Ks-Ek) limestones, grey to black, medium-thick bedded to massive bituminous locally microbrecciated and dolomitic in the upper members. Finally the oldest formation of this area is the Triassic–Upper Jurassic (Ts-Js.Kd) limestones, dolomitic limestones and dolomites. They constitute the base of the external zones tectonic nappe resulting in a local mylonitization at their base due tectonism. They are karstic, mainly in the upper members.

The map and the rose diagram of Figure 2 show that the fault zones of the study area are oriented NE-SW to NNE-SSW, NW-SE to NNW-SSE and E-W.

## **3. Methodology**

### **3.1. Geographic Information System (GIS)**

According to Goldfinger et al. (1994), shaded relief plots, contour plots, and wire-frame plots comprise the main tools to render the topography of an area. Detailed faulting tectonics and pattern deformation is better determined based on shaded relief plots (Oguchi et al., 2003). According to Kennely (2008), the illumination angle is also important for combined interpretation. Tectonic geomorphological interpretation is also supported by 3D view (Figure 3, Smith and Clark, 2005).

Digitization techniques and GIS were applied for mapping representation of the data. The digital elevation model (McGullagh, 1998; El-Sheimy et al., 2005) was created by the digitization of the topographic map contours (1:5,000 scale maps), while the cell size of the digital elevation model was 4 m. A spatial database was created and ArcGIS 9.3 software was used to process the collected data. This study was carried out using topographic maps of a scale of 1:5,000, published

by the Hellenic Army Geographical Service (H.A.G.S.). A Digital Elevation Model (DEM) was created by digitizing the contours with 2 m intervals and triangulation points of the above mentioned topographic maps.

GIS systems can generate many useful derivative datasets from topography. Two useful products for tectonics are slope and aspect maps. A slope map (Figure 4) assigns colours to the slope angle of each pixel of the elevation grid. This type of image may illuminate tectonic activity not apparent otherwise, and can be used to isolate ranges of topographic slope angles for statistical treatment, predictive capabilities of slope stability, or outcrop exposure. Similarly, an aspect map assigns colours to the azimuth of the slope direction (Figure 5). Both of these plots can be used for either topography or subsurface horizons to illuminate trends associated with deformation (Evans, 1972; Moellering and Kimerling, 1990; Brewer and Marlow, 1993). For the production of the slope angle layer, the DEM of the study area was used. The slopes were grouped in six classes: (i) < 5° (very gentle slopes), (ii) 5 – 10° (gentle slopes) (iii) 11 – 20° (intermediate slopes), (iv) 21 – 30° (moderately steep slopes), (v) 31 – 40° (steep slopes), and (vi) > 40° (very steep slopes) (Figure 4). As the aspect is the slope direction for a terrain, the aspect map was created from the DEM. The azimuth of the slope direction was grouped in nine classes: (i) -1° flat, (ii) 337.5 – 22.5° north, (iii) 22.5 – 67.5° northeast, (iv) 67.5 – 112.5° east, (v) 112.5 – 157.5° southeast, (vi) 157.5 – 202.5° south, (vii) 202.5 – 247.5° southwest, (viii) 247.5 – 292.5° west, (ix) 292.5 – 337.5° northwest .

### 3.2. Geomorphic Indices

Geomorphic indices are useful tools in evaluating tectonic activity, relating the sensitivity to rock resistance, climatic change and tectonic processes with the production of a certain landscape. The most useful indices are the mountain front sinuosity ( $S_{mf}$  index; Bull and McFadden, 1977) and the valley floor width to valley height ratio ( $V_f$  index; Bull, 1977, 1978).

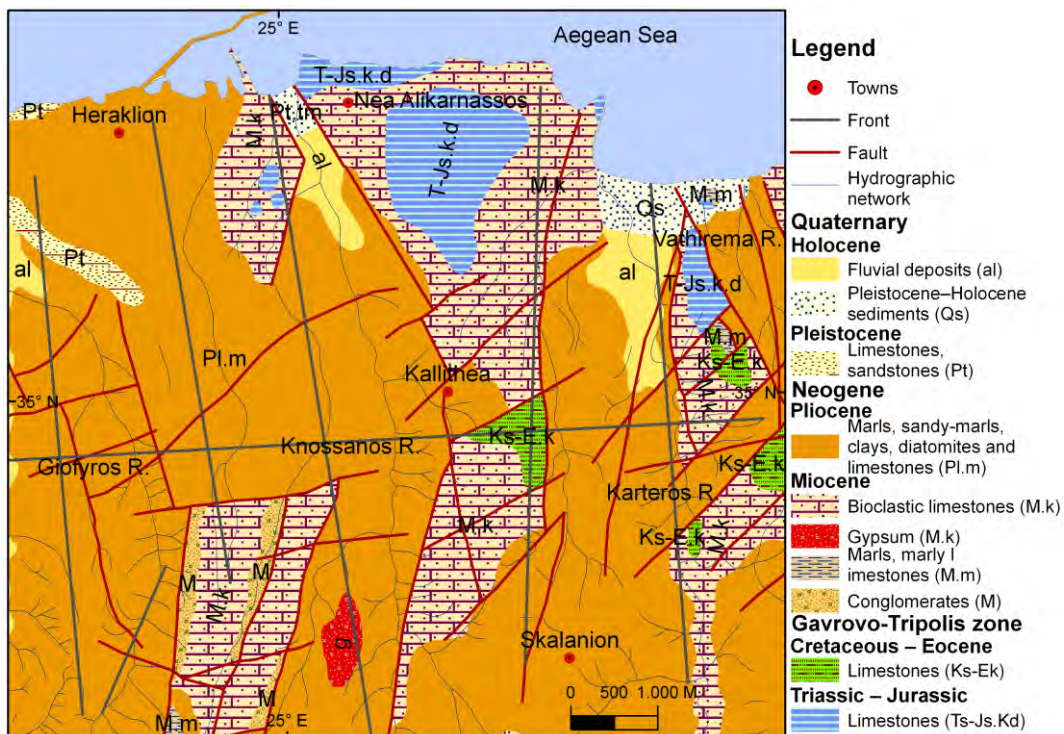
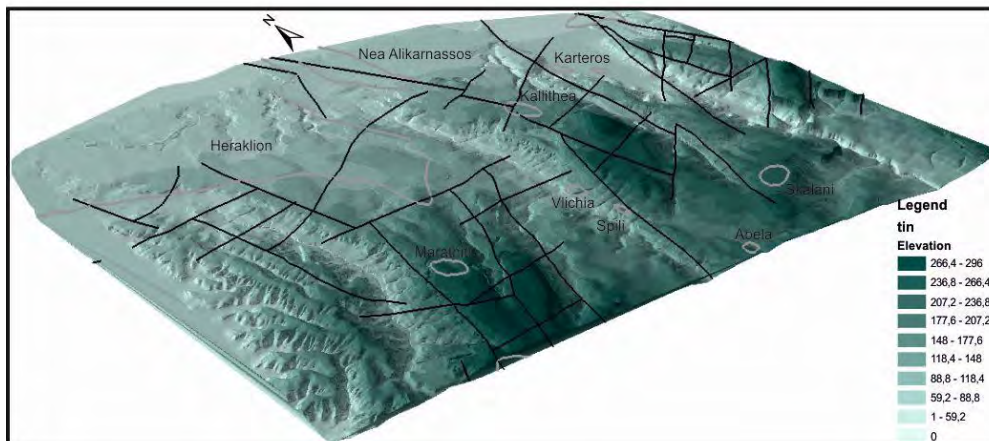
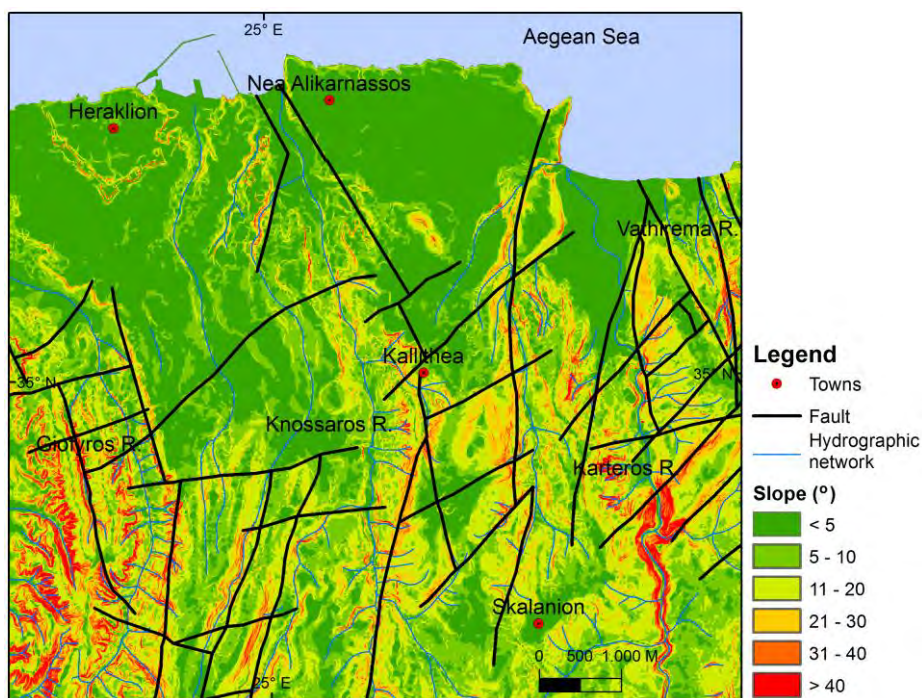


Figure 2 - Geological map of Heraklion (according to the geological map of IGME, Vidakis et al., 1996). The rose diagram (upper right) presents the orientation of the main faults.





**Figure 3 - 3D Topographic visualisation of the study area. Black lines correspond to faults.**



**Figure 4 - Slope map of the study area.**

Mountain front sinuosity is determined by measuring the length of the mountain front along the foot of the mountain  $L_{mf}$  and the straight line length of the mountain  $L_s$ . So, the mountain front sinuosity  $S_{mf} = L_{mf}/L_s$  is achieved (Bull and McFadden, 1977). The balance between erosion that tends to produce asymmetrical or sinuous fronts and tectonic forces that tend to create a straight mountain front coincident with an active range–bounding fault is presented by the above mentioned index. On the most tectonically active fronts, values of  $S_{mf}$  approach 1.0, whereas  $S_{mf}$  increases if the rate of uplift is reduced and erosional processes begin to form a front that becomes more irregular with time.  $S_{mf}$  values lower than 1.4 indicate tectonically active fronts (Rockwell et al., 1984; Keller, 1986; Burbank and Anderson, 2001) while higher  $S_{mf}$  values ( $>3$ ) are normally associated with inactive fronts in which the initial range–front fault may be more than 1Km away from the present erosional front (Bull and McFadden, 1977).

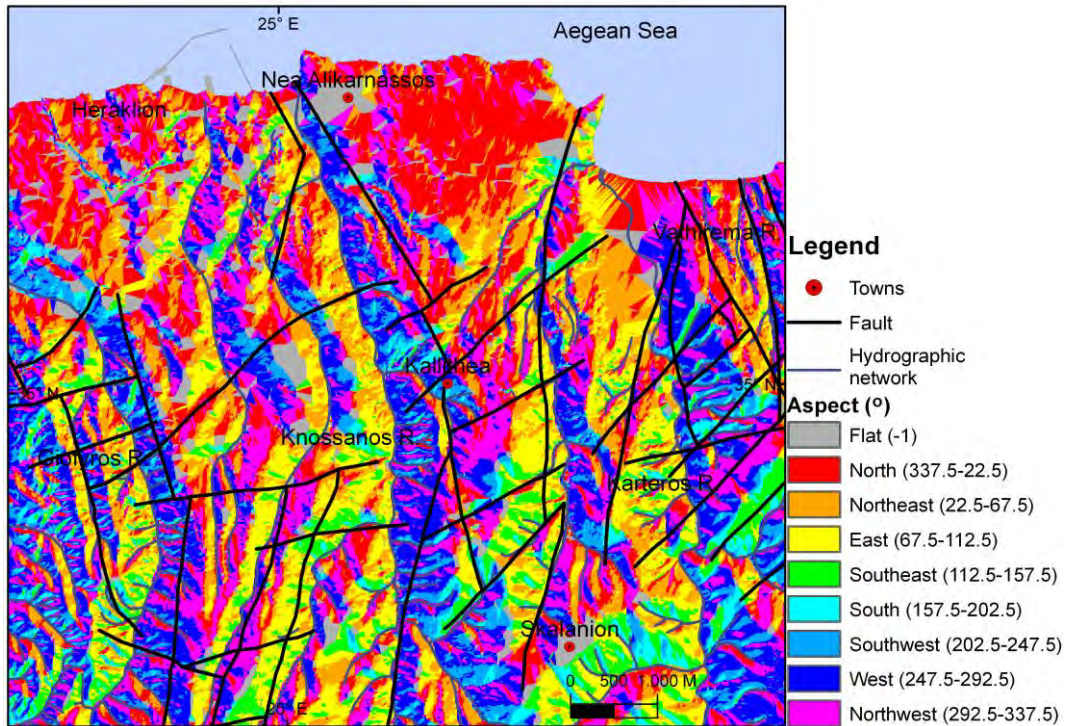


**Figure 5 - Aspect map of the study area.**

In this study, fronts are defined by a major fault bounded topographic range fronts with measurable relief exceeding two contour intervals (4m) in 1:5000 maps, which is the working scale used. The application of the Smf index was utilized in seven discrete segments (Figure 2), corresponding to major fault zones in the study area and taking into account similar geological and morphological characteristics especially concerning the drainage network. For the separation the following criteria were applied (Wells et al., 1988): a) intersection with large in scale cross-cutting drainage, relative to the front, b) abrupt changes in lithology (as it occurs in the western and eastern segments), c) changes in hill front orientation.

The Vf index reflects the difference between V-shaped valleys that are down cut in response to active uplift (low values of Vf) and broad-floored valleys that are eroding laterally into adjacent hill slopes in response to base level stability (high values of Vf) (Bull, 1978). The ratio of valley floor width to valley height (Vf) may be expressed as:

**Equation 1 - Ratio of Valley Floor Width to Valley Height**

$$Vf = \frac{2 \times Vf_w}{(E_{ld} - E_{sc}) + (E_{rd} - E_{sc})}$$

Where  $V_{fw}$  is the width of valley floor,  $E_{ld}$  and  $E_{rd}$  are elevations of the left and right valley divides, respectively, and  $E_{sc}$  is the elevation of the valley floor (Bull & McFadden, 1977). Comparison of the width of the floor of a valley with its mean height provides an index that indicates whether the stream is actively down cutting or is primarily eroding laterally into the adjacent hillslopes. The index reflects in this way differences between broad –floored canyons (U-shaped) with relatively high values of  $V_f$  and V-shaped canyons with relatively lower values (Keller, 1986).

#### 4. Results and Discussion

Morphological analysis of topographic features is often used for tectonic and structural studies. Digital elevation models (DEMs) and DEM analysis methods are used for fault recognition as about 90% of fault geomorphic indices can be defined quantitatively. At this point we have to mention that lithological contacts and intersection of bedding and topography, glacial features and wind erosion may also appear as lineaments in the derivative maps extracted from DEMs. So the use of indicated methods of DEMs analysis without geological data does not permit us to determine the fault morphology.

Slope and aspects superimposed by the faults and the drainage system are shown in Figures 4 and 5 respectively. The relief of the study area is mainly smooth with slopes ranging between 0 and 20°, while prevailing aspects are east, west, north and northwest. It is obvious that steep slopes (>30°) are mainly related to N-S, NNE-SSW and NNW-SSE oriented faulting. Additionally sudden changes corresponding to the azimuth of the slope direction are generally in agreement with the presence of steep slopes in the vicinity of the pre-mentioned faulting.

The influence of tectonism on the development of drainage system was examined by the comparison of fault and stream directions. As it is presented in Figures 4 and 5 the main channels of the drainage system of the study are parallel and generally oriented N-S. This direction is probably related to N-S, NNE-SSW and NNW-SSE oriented faulting. Regarding the low order streams of the drainage system, they develop directions mainly E-W, NE-SW and NW-SE. These stream directions have affected from E-W, NE-SW and NW-SE trending fault systems.

The values of the  $S_{mf}$  and  $V_f$  index were calculated for each front of the study area along with their trend and length (Table 1). Fronts were generally selected to be near or in the vicinity of major faults and/or near to rivers or streams. Fronts (1) and (2) are located in the western part of the study area in the vicinity of Giofyros river, while their lengths are 6.186 and 1.838Km respectively. Front (1) is partially parallel to faults trending mainly N-S to NNW-SSE while front (2) is sub-parallel to a fault trending NNE-SSW. Both fronts are mainly located in the Lower-Middle Pliocene (Pl.m) and Pleistocene sediments. The value of the  $S_{mf}$  corresponding to fronts (1) and (2) is 1.17 and 1.36 respectively, while the average value for  $V_f$  is 0.32 and 0.076.

Front (3) is located between Giofyros and Knossanos rivers being partially parallel to faults trending N-S to NNW-SSE and crosses the Upper Miocene formation (M.k) and the Lower-Middle Pliocene sediments (Pl.m). It is 5.513Km long. The value of the  $S_{mf}$  is 1.26 while the average value for  $V_f$  is 0.45.

Front (4) is almost parallel to Knossanos river trending N-S to NNW-SSE and it is 7.6Km long. It crosses the Triassic–Upper Jurassic (Ts-Js.Kd) limestones, the Upper Miocene formation (M.k) and the Lower-Middle Pliocene sediments (Pl.m) and finally the Pleistocene sediments (Pt.m). The value of the  $S_{mf}$  is 1.13 while the average value for  $V_f$  is 0.56.

Front (5) is located between Knossanos and Karteros rivers trending N-S to NNE-SSW and crosses the Cretaceous–Middle Eocene (Ks-Ek) limestones, the Upper Miocene formation (M.k) and the Lower-Middle Pliocene sediments (Pl.m). It is 6.64Km long. The value of the  $S_{mf}$  is 1.1 while the average value for  $V_f$  is 0.34.

Front (6) is almost parallel to Karteros river trending almost N-S and it is 5.75Km long. It crosses the Upper Miocene formation (M.k), the Lower-Middle Pliocene sediments (Pl.m), the Pleistocene – Holocene sediments (Qs) and the Holocene sediments (al). The value of the  $S_{mf}$  is 1.04 while the average value for  $V_f$  is 0.42.

Finally, front (7) is parallel to faults trending mainly E-W and it is 9.372Km long. It crosses the Cretaceous–Middle Eocene (Ks-Ek) limestones, the Upper Miocene formation (M.k), the Lower-Middle Pliocene sediments (Pl.m) and the Holocene sediments (al). The value of the  $S_{mf}$  is 1.26 while the average value for  $V_f$  is 0.44.

**Table 1** Values of geomorphological indices for the fronts (1-7) shown in Figure 2.

Front Num.	Location	Bounding rocks	Front trend	Front length (km)	S <sub>mf</sub>	Average V <sub>f</sub>
1	Giofyros	Pl.m, Pt, al	N-S	6.186	1.17	0.32
2	Giofyros	Pl.m	NNE-SSW	1.838	1.36	0.076
3	Between Giofyros and Knossanos	M.k, Pl.m	N-S	5.513	1.26	0.45
4	Knossanos	T-Js.kd, Mk, Pl.m, Pt.m	N-S	7.6	1.13	0.56
5	Between Knosanos and Karteros	Ks-E.k, M.k, Pl.m	NNE-SSW	6.64	1.1	0.34
6	Karteros	M.k, Pl.m, al, Qs	N-S	5.75	1.07	0.42
7	Giofyros-Karteros	Ks-E.k, M.k, Pl.m, al	E-W	9.372	1.26	0.44

The S<sub>mf</sub> values along the different fronts in the study area are generally varying between 1.07 and 1.36. As already mentioned, S<sub>mf</sub> values lower than 1.4 near or in the vicinity of faults, indicate tectonically active fronts (Rockwell et al., 1984; Keller, 1986; Burbank and Anderson, 2001). The fronts generally cross Miocene - Pliocene sediments, showing approximately the same resistance to the erosion. The low S<sub>mf</sub> values (close to 1) indicate that the area is affected by tectonic activity rather than erosion processes.

Similarly, V<sub>f</sub> index values are low ranging between 0.076 and 0.56. According to Silva et al (2003) values of V<sub>f</sub> < 1.0 express the develop of V-shaped valleys indicating tectonic activity. Both index values suggest that the involved fault systems fall under the category of Class-I, representing high tectonic activity.

## 5. Conclusions

In the present study morphological and geomorphotectonic analysis are combined in order to determine the impact of the tectonic activity in the Heraklion area.

DEM analysis methods are used for fault recognition but the use of these methods without geological data does not permit to determine the fault morphology. The analysis of the morphological features indicated that steep slopes (>30°) and sudden changes corresponding to the azimuth of the slope direction are mainly related to N-S, NNE-SSW and NNW-SSE oriented faulting.

The comparison of the fault and stream directions suggests the influence of the tectonic activity on the drainage system. The main channel directions of the drainage system are mainly related to faults striking N-S, NNE-SSW and NNW-SSE. The E-W, NE-SW and NW-SE trending fault systems controls the low order streams. Geomorph indices, used in the present study, are the mountain front sinuosity index (S<sub>mf</sub>) and the valley floor/width ratio index (V<sub>f</sub>). The S<sub>mf</sub> and V<sub>f</sub> values are low, indicating that the active tectonism influences the geomorphological evolution of the study area.



## 6. Acknowledgements

We would like to thank Assoc. Professor Rondoyanni Th. and Dr. Chatzipetros A. for their critical reviews, which help improved the manuscript.

## 7. References

- Bathrellos G.D., Antoniou V.E. and Skilodimou H.D. 2009. Morphotectonic characteristics of Lefkas Island during the Quaternary (Ionian Sea, Greece), *Geologica Balcanica*, 38(1-3), 23-33.
- Brewer C.A. and Marlow K.A., 1993. Computer representation of aspect and slope simultaneously, *Proc. of the 11th International Symposium on Computer- Assisted Cartography (Auto-Carto-11)*, Minneapolis, Minnesota, 328–337.
- Bull W. 1977. Tectonic geomorphology of the Mojave Desert, *U.S. Geol. Surv. Contact Rep.* 14–08–001–G–394, Office of Earthquakes, Volcanoes and Engineering, Menlo Park, Calif., 188.
- Bull W. 1978. Geomorphic tectonic activity classes of the south front of the San Gabriel Mountains, California, *U.S. Geol. Surv. Contact Rep.* 14–08–001–G–394, Office of Earthquakes, Volcanoes and Engineering, Menlo Park, Calif., 59.
- Bull W. and McFadden L. 1977. Tectonic geomorphology north and south of the Garlock Fault, California, *Geomorphology in Arid regions*, in Doehring, D.O., ed., *Publications in Geomorphology*, State University of New York at Binghamton, 115–138.
- Burbank D.W. and Anderson R.S. 2001. *Tectonic geomorphology*, Blackwell Science, Inc. USA.
- El-Sheimy, N., Valeo, C., Habib, A., 2005. *Digital Terrain Modeling: Acquisition, Manipulation and Applications*, Artech House Publishers, Boston. 270 pp.
- Evans I. 1972. General geomorphometry, derivatives of altitude and descriptive statistics. In Chorley, R.J., ed., *Spatial Analysis in Geomorphology: Harper and Row*, New York, 17–90.
- Fassoulas C. 1999. The structural evolution of Central Crete: insight into the tectonic evolution of the South Aegean (Greece), *J. Geodynam.*, 27, 23-43.
- Goldfinger C., Kulm L.D., Yeats R.S., McNeill L.C. and Hummon C. 1997. Oblique strike-slip faulting of the central Cascadia submarine forearc, *Journal of Geophysical Research*, 102, 8217-8243.
- Jolivet L., Goffé B., Monie P., Truffert-Luxey C., Patriat M. and Bonneau M. 1996. Miocene detachment on Crete and exhumation P-T-t paths of high-pressure metamorphic rocks. *Tectonics*, 15, 1129-1153.
- Kamberis E., Bathrellos G., Kokinou E. and Skilodimou H. 2012. Correlation between the structural pattern and the development of the drainage network in the area of Western Thessaly basin (Greece), *Central European Journal of Geosciences*, 4(3), 416-424, doi: 10.2478/s13533-011-0074-7.
- Keller E. 1986. Investigation of active tectonics: use of surficial earth processes. In Wallace, R. E., eds, *Active Tectonics studies in Geophysics*, Nat. Acad. Press, Washington, DC, 136–147.
- Kennely P.J. 2008. Terrain maps displaying hill-shading with curvature, *Geomorphology*, 102, 567–577.
- Kilias A., Fassoulas C. and Mountrakis D., 1994. Tertiary extension of continental crust and uplift of Psiloritis metamorphic core complex in the central part of the Hellenic Arc (Crete,Greece), *Geol. Rundsch.*, 83, 417-430.
- Kokinou E., Alves T. and Kamberis E. 2012. Structural decoupling on a convergent forearc setting (Southern Crete, Eastern Mediterranean), *Geol. Soc. Am. Bulletin*, 124(7/8), 1352–1364, doi:10.1130/B30492.1.
- McCullagh M.J. 1998. Quality, use and visualisation in terrain modeling. In: Lane, S.N., Richards, K.S., Chandler, J.H. (Eds.), *Landform Monitoring, Modeling and Analysis*, John Wiley & Sons, Chichester, 95–117.

- Moellering H., Kimerling and A.J. 1990. A new digital slope-aspect display process, *Cartography and Geographic Information Systems*, 17, 151–159.
- Oguchi T., Aoki T. and Matsuta N. 2003. Identification of an active fault in the Japanese Alps from DEM-based hill shading, *Computers and Geosciences*, 29, 885–891.
- Riquelmea R., Martinod J., Herail G., Darrozesa J. and Charrierb R. 2003. A geomorphological approach to determining the Neogene to Recent tectonic deformation in the Coastal Cordillera of northern Chile (Atacama), *Tectonophysics*, 361, 255–275.
- Rockwell T., Keller E. and Johnson D. 1984. Tectonic geomorphology of alluvial fans and mountain fronts near Ventura, California, in Morisawa, M., Hack T. J., eds., *Tectonic Geomorphology*, Publ. In *Geomorphology*, State University of New York, Binghamton, 183–207.
- Silva P.G., Goy J.L., Zazo C. and Bardají T. 2003. Fault-generated mountain fronts in southeast Spain: geomorphologic assessment of tectonic and seismic activity, *Geomorphology*, 50, 203–225.
- Smith M.J. and Clark C.D. 2005. Methods for the visualization of digital elevation models for landform mapping, *Earth Surface Processes and Landforms*, 30, 885–900.
- Theocharis D. and Fountoulis I. 2002. Morphometric indices and tectonically active structures: the case of Salamis island, *Proc. of the 6<sup>th</sup> Panhellenic Geographical Congress*, *Geogr. Soc. Greece*, I, 97-106, (in Greek with English abstract).
- Tsodoulos I., M. Koukouvelas I. K. and Pavlides S. 2008. Tectonic geomorphology of the easternmost extension of the Gulf of Corinth (Beotia, Central Greece), *Tectonophysics*, 453, 211–232.
- Wells S.G., Bullard T. F., Menges C. M., Drake P. G., Karas P. A., Kelson, K. I., Ritter, J. B. and Wesling J. R. 1988. Regional variations in tectonic geomorphology along a segmented convergent plate boundary, Pacific coast of Costa Rica, *Geomorphology*, 1, 239–265.
- Vidakis M., Meulenkamp J.E., Koutsouveli A., Ioakim Ch., Papazeti E. and Skourtsi-Koronaïou V. 1996. *Geological Map of Greece* in 1:50,000 scale – Heraklion Sheet. IGME, Athens.
- Zachariasse W.J., van Hinsbergen, D.J.J. and Fortuin, A.R. 2011. Formation and fragmentation of a late Miocene supradetachment basin in central Crete: implications for exhumation mechanisms of high-pressure rocks in the Aegean forearc, *Basin Res.*, 23, 678–701, doi: 10.1111/j.1365-2117.2011.00507.x.